

## Soft X-ray Spectroscopy of the Hot DA White Dwarf LB1919 and the PG1159 Star PG1520+525

K. Werner,<sup>1</sup> J. J. Drake,<sup>2</sup> T. Rauch,<sup>1</sup> S. Schuh,<sup>3</sup> and A. Gautschy<sup>4</sup>

<sup>1</sup>*Institut für Astronomie und Astrophysik, Universität Tübingen, Sand 1, 72076 Tübingen, Germany*

<sup>2</sup>*Harvard-Smithsonian Center for Astrophysics, MS 3, 60 Garden Street, Cambridge, MA 02138, USA*

<sup>3</sup>*Institut für Astrophysik, Universität Göttingen, Friedrich-Hund-Platz 1, 37077 Göttingen, Germany*

<sup>4</sup>*Wetterchrüzstr. 8c, 4410 Liestal, Switzerland*

**Abstract.** We have performed soft X-ray spectroscopy of two hot white dwarfs with the *Chandra* observatory using the *Low Energy Transmission Grating*. The first target is the hot DA white dwarf LB1919 ( $T_{\text{eff}}=69\,000$  K). This star is representative of a small group of hot DAs whose metallicities lie well below predictions from radiative levitation theory. The *Chandra* spectrum shows a rich absorption line spectrum which may allow to find the origin of the low-metallicity nature of these DAs. The second target is PG 1520+525, a very hot non-pulsating PG1159 star. We find that it is hotter ( $T_{\text{eff}}=150\,000$  K) than the pulsating prototype PG 1159–035 ( $T_{\text{eff}}=140\,000$  K) and conclude that both stars confine the blue edge of the GW Vir instability strip.

### 1. The hot DA white dwarf LB1919

The purity of WD atmospheres results from gravitational settling of heavy elements. The lightest element, either hydrogen or helium, is floating on top of the star, giving rise to the DA and non-DA spectral classes, respectively. Hydrogen in hot DA atmospheres is almost completely ionized so that the EUV/soft X-ray opacity is strongly reduced. As a consequence, DAs with  $T_{\text{eff}} > 30\,000$  K can emit detectable amounts of thermal soft X-ray radiation, leaking out from deep, hot photospheric layers.

The *ROSAT* all-sky survey, however, detected *many* fewer white dwarfs ( $< 200$ ) than expected ( $> 5000$ ) – X-ray emission turned out to be the exception rather than the rule. It was realized that additional absorbers must be present in the atmospheres. *ROSAT* and *EUVE* observations revealed that metals are the origin of this additional opacity, and that the EUV spectral flux distribution of hot DAs is most strongly determined by iron and nickel through their enormously large number of absorption lines. Radiative levitation can keep traces of these and other metals floating in the atmosphere against gravitational pull (e.g. Chayer et al. 1995): *the metal abundances therefore generally increase with increasing  $T_{\text{eff}}$* . As a consequence, only very few DAs with  $T_{\text{eff}} > 60\,000$  K were detected in the *EUVE* and *ROSAT* all-sky surveys because the increasing EUV opacity is effectively blocking flux.

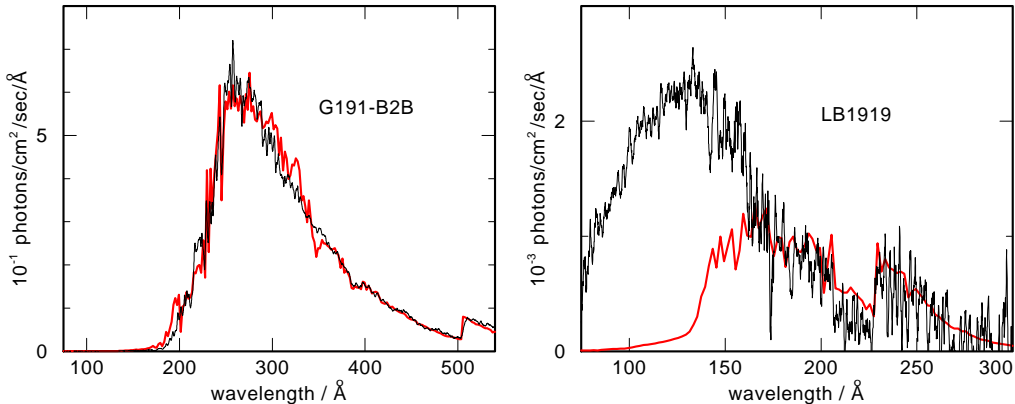


Figure 1. *EUVE* spectra of two hot DA white dwarfs (thin lines) compared to spectra from models (thick lines) which consider gravitational settling and radiative levitation. **Left:** The model fit to G191-B2B is very good. **Right:** The observed flux of LB1919 at  $\lambda < 150 \text{ \AA}$  is much higher than predicted by the model. For an unknown reason, the metallicity in LB1919 is peculiarly low.

A breakthrough in understanding WD atmospheres has been the successful development of self-consistent models which describe the vertical stratification of element abundances by assuming equilibrium between gravitation and radiative acceleration. These models no longer have the surface metal abundances as free parameters: they are instead computed on physical grounds. Generally, good agreement is obtained between observed and computed EUV flux distributions (Schuh et al. 2002). However, several exceptions are known. Some DAs show much larger metal abundances than expected from theory. This has been explained by either accretion from the ISM or wind-accretion from unseen companions.

Much more difficult to explain are those objects whose metallicity is *smaller* than expected from radiative levitation theory. One prominent example is the famous white dwarf HZ43 ( $T_{\text{eff}}=51\,000 \text{ K}$ ) whose atmosphere is virtually metal free and shows no EUV or X-ray absorption features. Even more surprising is the low metallicity of DAs with even higher temperatures. One of the hottest known DAs, LB1919 ( $T_{\text{eff}}=69\,000 \text{ K}$ ), has extraordinarily low metal abundances.

LB1919 is the hottest DA of the 90 detected in the *EUVE* all-sky survey (Vennes et al. 1997), and of the 20 DAs for which *EUVE* spectra have been analysed in detail by Wolff et al. (1998). The chemical composition is not known: since the *EUVE* spectral resolution is insufficient to unambiguously identify lines from individual species, the metallicity of fainter DAs is usually determined relative to that of the well-studied DA G191-B2B ( $T_{\text{eff}}=56\,000 \text{ K}$ ). Unlike LB1919, G191-B2B is sufficiently bright and metal-rich that its surface composition can be constrained through UV spectroscopy. Our stratified models successfully describe in detail the EUV-UV spectrum of G191-B2B (Fig. 1). The

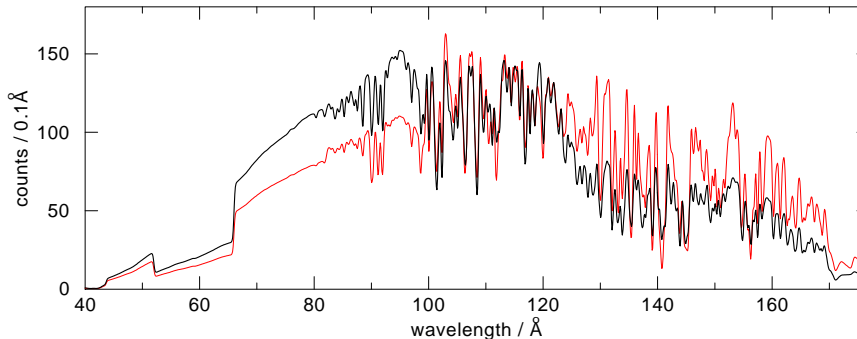


Figure 2. Simulated *Chandra* spectra of LB1919 with homogeneously mixed models. Model parameters are  $T_{\text{eff}}=70\,000$  K,  $\log g=8.2$ . Following the *EUVE* analysis of Wolff et al. (1998), the Fe and Ni abundances are 10% of the abundances determined for G191-B2B, i.e.,  $\text{Fe}/\text{H}=7.5 \cdot 10^{-7}$  and  $\text{Ni}/\text{H}=5 \cdot 10^{-8}$ . In order to demonstrate the sensitivity of the spectrum against abundance variations, we show two models. The first has Ni increased by 1 dex (thick line), the second Fe and Ni increased by 1 dex (thin line).

*EUVE* spectra of other DAs could also be fitted by simply scaling this relative metal abundance pattern.

The *EUVE* spectrum of LB1919, however, cannot be explained by spectral models based on homogeneous abundances scaled relative to G191-B2B, and stratified models including radiative levitation fail spectacularly (Fig. 1). Its EUV spectrum suggests a surprisingly low metallicity – approximately 10% of that of G191-B2B, despite being significantly hotter. The failure to match *EUVE* spectra is due to either the assumed G191-B2B-like abundance pattern being wrong, or due to a different stratification than predicted by pure radiative levitation.

Several processes could disturb the equilibrium between gravitation and levitation and are potentially responsible for the metal-poor hot DAs: mass-loss; accretion from the ISM; convection, and mixing through rotation. Mass-loss would have the effect of homogenising a chemical stratification, but it also has been shown that mass-loss rates drop below the critical limit ( $10^{-16} M_{\odot}/\text{yr}$ ) for DAs cooler than 70 000 K so that this phenomenon should not occur in hot DAs like LB1919 (Unglaub & Bues 1998). Wind accretion calculations show that accretion is prevented for LB1919 since its luminosity is  $> 1 L_{\odot}$ ; instead a mass-loss rate of  $\approx 10^{-18} M_{\odot}/\text{yr}$  will be sustained (MacDonald 1992). Convection would homogenise abundances; however, the atmosphere of LB1919 is convectively stable because hydrogen is almost completely ionised. Rotation could lead to mixing through meridional currents, but most WDs are very slow rotators and analysis of a *FUSE* archival spectrum of LB1919 shows deep and sharp Lyman line cores which clearly excludes such a high rotation rate. To summarize, there is currently no explanation for the very low metallicity in LB1919 and similar DAs.

In order to find out if the metals in the atmospheres of these peculiar low-metallicity white dwarfs are stratified or homogeneous we decided to perform

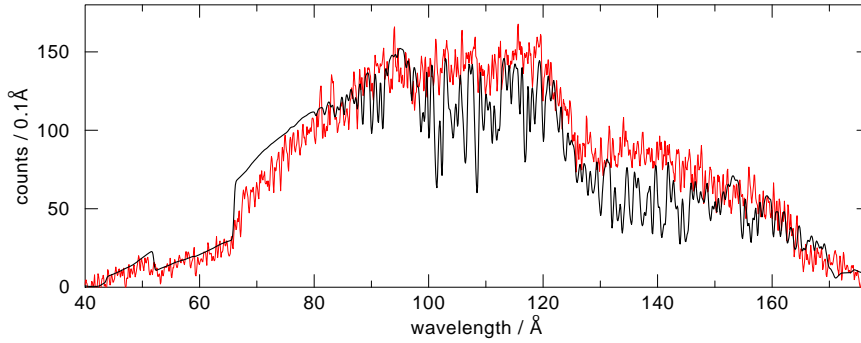


Figure 3. *Chandra* spectrum of LB1919 (thin line). Overplotted is one of the model spectra depicted in Fig. 2 (Ni 10 times enhanced, Fe on the Wolff et al. value). The line features in the model are stronger than observed.

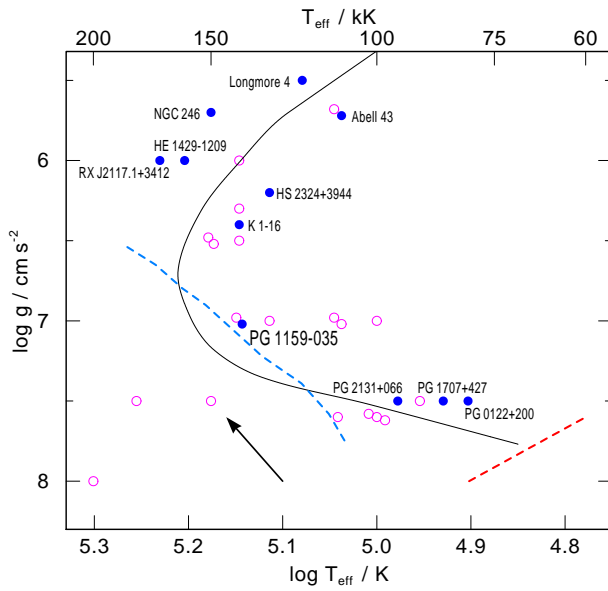


Figure 4. The pulsating PG1159 stars (filled symbols with name-tags) and the non-pulsators. The non-pulsator PG 1520+525 is marked by an arrow. The dashed lines are theoretical blue and red edges of the instability strip from Gautschi et al. (2005) and Quirion et al. (2004), respectively. Also shown is a  $0.6 M_{\odot}$  post-AGB track (full line) from Wood & Faulkner (1986).

*Chandra* spectroscopy of LB1919 with the *Low Energy Transmission Grating* (LETG/HRC-S). It was demonstrated by Vennes et al. (2002) that individual lines can in principle be identified in *Chandra* spectra of hot DAs (GD246). A simulation with our model spectra shows that we should also be able to identify individual lines in LB1919 (Fig. 2). In Fig. 3 we show the observed spectrum.

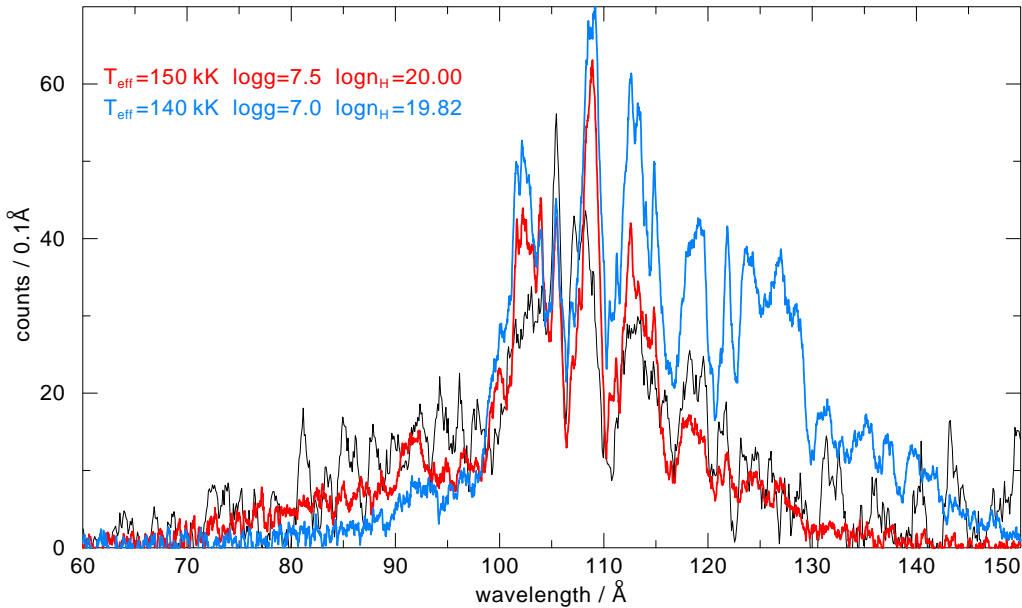


Figure 5. *Chandra* spectrum of PG 1520+525 (thin line), smoothed with a  $0.5 \text{ \AA}$  boxcar, and simulated observations from two models with different  $T_{\text{eff}}$ . The 140 kK model overestimates the flux at  $\lambda > 110 \text{ \AA}$ . The models represent the pulsator–non-pulsator pair, see Tab. 1 for atmospheric parameters.

It was taken on Feb. 02–03, 2006, with an integration time of 111 ksec, and it clearly shows many spectral lines. The overplotted spectrum of our preliminary model reproduces the spectral shape, however, the absorption lines are obviously too strong.

## 2. The PG1159 star PG 1520+525

PG1159 stars are hot H-deficient (pre-) WDs which are probably the outcome of a late He-shell flash (Werner & Herwig 2006). The pulsating members of this spectral class form the GW Vir instability strip in the HRD. In order to constrain stellar evolutionary models it is of interest to empirically find the edges of this strip. The pulsating prototype PG 1159–035 and the non-pulsator PG 1520+525 are located close to each other in the  $g$ – $T_{\text{eff}}$  plane (Fig. 4) and it can be argued that the blue edge of the strip is constrained by this pair of stars. From optical and UV spectroscopy it was found that PG 1520+525 is indeed hotter than PG 1159–035 ( $150\,000 \pm 15\,000 \text{ K}$  and  $140\,000 \pm 5\,000 \text{ K}$ , respectively), however, the error bars of the analyses overlap considerably. While we could constrain the temperature of PG 1159–035 with high precision (Jahn et al. 2007), the uncertainty for PG 1520+525 is still very large (Dreizler & Heber 1998).

We have taken a *Chandra* LETG/HRC-S spectrum because our models predict a strong sensitivity of the soft-X-ray flux to variations in  $T_{\text{eff}}$ . The observation was performed on April 04–06, 2006, with an integration time of

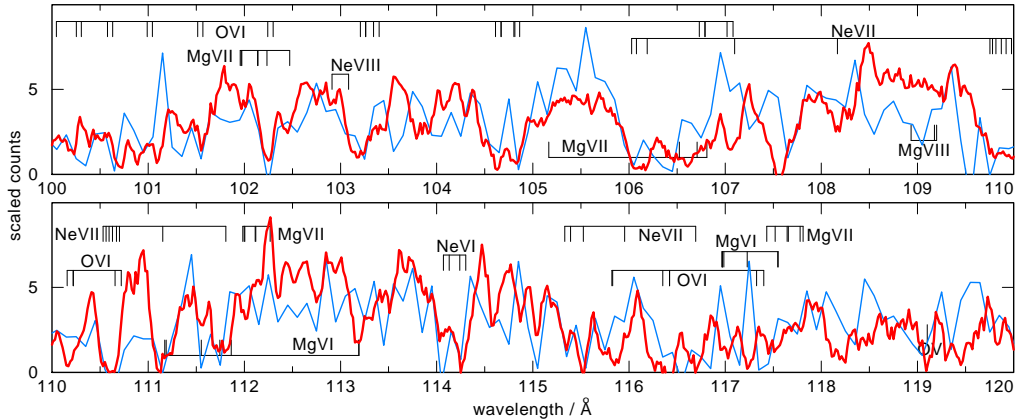


Figure 6. Detail of the *Chandra* spectrum of PG 1520+525 (thin graph) and our 150 kK simulation. Lines from O VI and Ne VI/VII can be identified.

Table 1. Atmospheric parameters of the pulsator–non-pulsator pair. Abundances are given in mass fractions.

	PG 1159–035	PG 1520+525
$T_{\text{eff}}/\text{K}$	140 000	150 000
$\log g$	7.0	7.5
He	0.33	0.43
C	0.48	0.38
O	0.17	0.17
Ne	0.02	0.02
$\log F$	–5.5	–4.0
$\log N$	–3.0	< –3.0

142 ksec. We show the spectrum in Fig. 5 together with two models of different temperature. There is evidence that the hotter model fits much better and we hope that a detailed analysis will give  $T_{\text{eff}}$  with a precision of  $\pm 5000$  K. This analysis requires to fit individual features in the spectrum. Fig. 6 shows that we can identify a number of absorption lines from highly ionised oxygen and neon. At present it seems that we can confirm that PG 1520+525 and PG 1159–035 do indeed constrain the blue edge of the GW Vir instability strip. The interpretation of our results, however, must consider that the exact position of the edge is depending on the photospheric composition (Quirion et al., these proceedings).

**Acknowledgments.** T.R. was supported by DLR grant 50 OR 0201. J.J.D. was supported by NASA contract NAS8-39073 to the *Chandra X-ray Center*.

## References

- Chayer, P., Fontaine, G., & Wesemael, F. 1995, *ApJS*, 99, 189  
 Dreizler, S., & Heber, U. 1998, *A&A*, 334, 618  
 Gautschy, A., Althaus, L. G., & Saio, H. 2005, *A&A*, 438, 1013  
 Jahn, D., Rauch, T., Reiff, E., Werner, K., Kruk, J. W., & Herwig, F. 2007, *A&A*, in press (available on astro-ph)  
 MacDonald, J. 1992, *ApJ*, 394, 619  
 Quirion, P. O., Fontaine, G., & Brassard, P. 2004, *ApJ*, 610, 436

- Schuh, S.L., Dreizler, S., & Wolff, B. 2002, *A&A*, 382, 164  
Unglaub, K., & Bues, I. 1998, *A&A*, 338, 75  
Vennes, S., Thejll, P.A., Genova Galvan, R., & Dupuis, J. 1997, *ApJ*, 480, 714  
Vennes, S., & Dupuis, J. 2002, in *The High Energy Universe at Sharp Focus*, ASP Conf. Series, 262, 57  
Werner, K., & Herwig, F. 2006, *PASP*, 118, 183  
Wolff, B., Koester, D., Dreizler, S., & Haas, S. 1998, *A&A*, 329, 1045  
Wood, P. R. & Faulkner, D. J. 1986, *ApJ*, 307, 659